Proceedings of the 7th International Conference on Astrodynamics Tools and Techniques (ICATT),
6-9th November 2018, Oberpfaffenhofen, Germany.
https://indico.esa.int/event/224/contributions/4010/

NEAR RECTILINEAR ORBITS AROUND THE MOON AS OPERATIONAL ORBIT FOR THE FUTURE DEEP SPACE GATEWAY

Carlos Sánchez Lara, Joan Pau Sánchez Cuartielles

Cranfield University, Cranfield, England MK43 0AL, United Kingdom

ABSTRACT

The aim of this paper is to revise the suitability of Near-Rectilinear Halo Orbits (NRHOs) as long-term destinations for a new crew-tended space station; referred here as Deep Space Gateway (DSG). NRHOs are a subset of the halo families characterized by promising stability properties. The document presents the formal definition and identification of NRHOs, as in the CR3BP model. Dynamical substitutes of the NRHOs are also refined in the Bi-Circular Model (BCM) by means of a multiple shooting method. Key features such as lunar south-pole coverage, station keeping requirements and accessibility of the orbit are then analysed. Several maintenance strategies based on three different underlying principles are considered and, finally, the accessibility of NRHOs from the Earth and polar Moon orbits is investigated.

Index Terms— NRHO, DSG, Station keeping, Cislunar space, Differential corrections

1. INTRODUCTION

A renewed vision to send humans beyond Low Earth Orbit (LEO) has given rise to a whole range of studies proposing different destinations and operational orbits for a new crew-tended space station; initially known as Deep Space Gateway (DSG). The DSG is envisaged as a staging location for lunar exploration and a gateway to interplanetary space [1]. However, the station will serve multiple additional purposes (not yet defined), including scientific observations or space environment analyses among others [2]. Therefore, a fixed destination for the DSG has not been designated. In fact, it is expected that the station will perform excursions between different useful orbits over its service life [3]. However, a potential destination for extended periods is required that should meet the following set of requirements:

- Excellent lunar poles coverage. In particular, the south pole should be targeted, since it is the focus of current studies as a result of the availability of potentially water-rich regions and constant exposure to sunlight.
- A suitable orbit should not require high station keeping costs and risks associated with getting into escape trajectories should be minimised. Given the short timescales in the Earth-Moon system, misleading monitoring information or missing station keeping manoeuvres could lead a spacecraft into a diverging path within a few days.
- Accessibility to and from the orbit is also a key driver requirement. Access to the lunar poles is crucial to facilitate lunar exploration and efficient transfers from terrestrial orbits are mandatory.

NRHOs comply with these specifications and have been identified as one of the most promising destinations for the DSG [1]. A general study of NRHOs is presented in this paper to get a clear insight into their behaviour.

Multiple missions in the Sun-Earth system and just a few in the Earth-Moon system have successfully carried out station keeping manoeuvres near the libration points [4]. However, no spacecraft has ever been placed into an NRHO [5], and no station keeping algorithms have undergone extensive analysis for this type of orbits. One objective of this study is the analysis and adaptation of station keeping strategies proposed in the literature for successfully tested trajectories ([6], [7], [8]) to missions in NRHOs. Apart from efficient, in terms of ΔV costs, and reliable, a computationally cheap methodology is sought, which would be beneficial for onboard implementation.

As an attempt to validate the accessibility of NRHOs, the paper also investigates the natural flow associated with these orbits in search for low-cost trajectories through the exploitation of their invariant manifolds in the CR3BP.

2. DYNAMICAL MODELS

Throughout this investigation, force models that provide different levels of fidelity have been considered; the Circular Restricted Three-Body Problem (CR3BP) and the Bi-Circular Model (BCM).

2.1. Circular Restricted Three-Body Problem

The initial design phases of orbits and transfer trajectories require a vast understanding of the dynamics that govern the motion of the spacecraft. Despite not yielding a closed-form solution, the CR3BP provides an autonomous approximation to the dynamics of the problem. The CR3BP is a particular case of the Three-Body Problem where the spacecraft's

acceleration is dominated by the gravity field of two primary bodies (Earth and Moon in this case), which move in circular coplanar orbits around their common barycentre. Apart from its simplicity, this model is the one that allows the generation of certain closed periodic trajectories such as halo orbits, which are the focus of this study.

For convenience, quantities in this system are nondimensionalized such that the mean motion of the main bodies, as well as the distance between them, are both equal to unity. The Earth and Moon have nondimensional masses equal to $1-\mu$ and μ, respectively, where μ is the mass parameter of the system. Using a barycentric reference system and a dimensionless set of units, the equations of motion can be found in [9].

2.2. Bi-Circular Model

Despite being an accurate approach, for some studies to be reliable, it is appropriate to validate the preliminary results obtained in the CR3BP with higher fidelity models. A clear example is the case of station keeping analyses in the cislunar space. In the Earth-Moon CR3BP, the attraction of the Sun is one of the most important perturbations acting on a spacecraft [9], and not accounting for this celestial body can conduce to misleading orbit maintenance predictions. For that reason, a simplified four-body problem is employed for the computation of station keeping costs; the BCM.

The BCM is a closer approach to the real dynamical environment than the CR3BP but still maintains a low level of complexity and computational cost. The main assumptions are; the Earth and the Moon move in circular orbits around their barycentre, and the Earth-Moon barycentre, in turn, moves in a circular orbit around the Sun-Earth-Moon centre of masses. Gómez et al. [10] presents the BCM equations of motion relative to the rotating Earth-Moon system.

3. NEAR-RECTILINEAR HALO ORBITS

In the Earth-Moon system, Near Rectilinear Halo Orbits (NRHOs) are a subset of the halo families characterized by a close passage over the polar regions of the Moon and tend toward almost rectilinear orbits as seen in the x-z plane, from which NRHOs take their name (Figure 1).

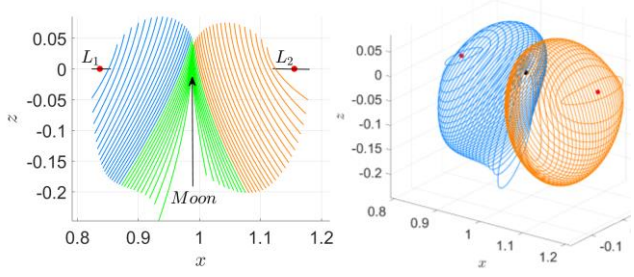

Figure 1. L_1 and L_2 southern halo families. In the x-z view (left), the green line corresponds with the NRHOs and the black line identifies planar halo orbits (bifurcation from Lyapunov orbits).

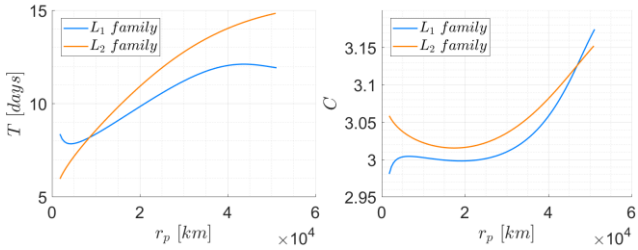

Figure 2. Period (left) and Jacobi constant (right) of L_1 and L_2 halo families.

Halo orbits are commonly classified according to their perilune [11], denoted by r_p. Relevant parameters of the L_1 and L_2 families are represented as a function of r_p in the next figures. The period of the orbit is a useful parameter for the initial design phase of a mission. Especially, they play an important role when the Sun perturbation is considered, due to the resonance between orbits. Typical periods of halo orbits in the Earth-Moon system range from 1 to 2 weeks, approximately. This variable is exposed in Figure 2 (left).

The Jacobi constant (C) associated with each family is shown in Figure 2 (right). Generally, the larger the r_p, the higher the C and, therefore, the lower the energy that corresponds to it.

3.1. Stability: Formal Identification of NRHOs

In the literature, NRHOs' boundaries are usually delineated according to their linear stability [11]. It is found that the eigenstructure of the monodromy matrix of the system can be used to identify the unstable character of an orbit [12]. The eigenvalues (λ) can be associated with different subspaces according to their magnitude; the existence of eigenvalues larger than one would imply an unstable periodic orbit. Therefore, a useful parameter to characterise the linear stability of an orbit is the so-called stability index, ν. In [13], it is defined using the following expression,

$$\nu = \frac{1}{2}\left(\lambda_{max} + \frac{1}{\lambda_{max}}\right) \qquad (1)$$

Where λ_{max} is the length of the eigenvalue with the maximum magnitude of the monodromy matrix. In Figure 3, the stability index of the L_1 and L_2 halo families as a function of their periapsis is shown.

Considering the definitions of stable, unstable and centre subspaces, it is clear that, the higher the stability index, the more unstable is the orbit. Therefore, large ν's imply that a trajectory would diverge from the reference orbit quickly. On the other hand, if $\nu = 1$ (minimum value), the orbit is marginally stable according to the linear analysis. It should be noted that eigenvalues are constant along the periodic orbits, so, the stability index can be used to characterise them. There exists a region where ν is constrained between 1 and 3,

approximately, which corresponds to the region of small r_p. This zone of Figure 3 (top) has been zoomed in in Figure 3 (bottom). As it can be seen, several transitions between unstable ($\nu > 1$) and marginally stable ($\nu = 1$) orbits exist. In this paper, and for the Earth-Moon system, NRHOs are defined as the members of the halo families that range from a periapsis equal to the Moon radius ($1737\ km$) to the r_p corresponding with the last stability transition, from which ν becomes increasingly unstable.

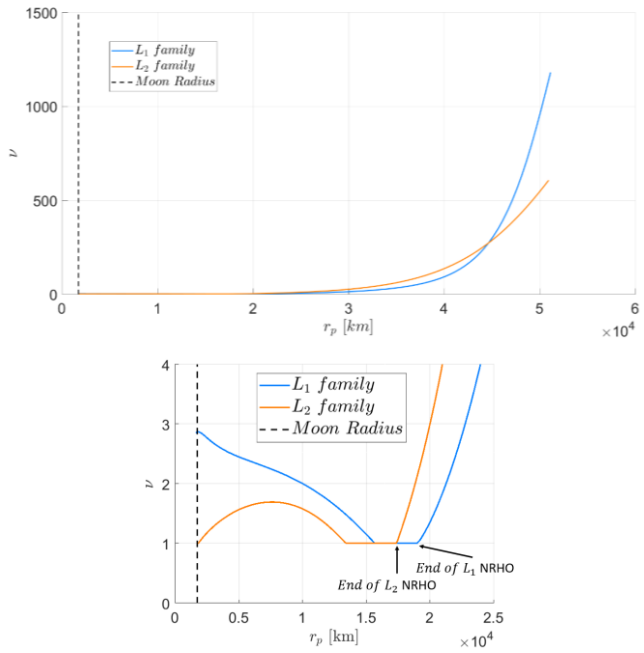

Figure 3. Stability indices of L_1 and L_2 halo families. The region of NRHOs has been zoomed in (bottom), which ranges from $r_p = 1737$ to $r_p \approx 20{,}000\ km$.

3.1. Dynamical Substitutes

Halo orbits have been defined as three-dimensional periodic orbits near the libration points of a three-body system. As mentioned before, it is necessary to assess the trajectories in higher fidelity models. The problem is, when a periodic orbit is calculated in the CR3BP and then propagated in a four-body problem, the periodicity of this orbit is lost. In addition, it has been demonstrated that halo orbits are generally unstable, and some station keeping strategy is required to keep the motion bounded, even in the CR3BP. While the station keeping costs would be very low in the three-body problem, forcing the path of a spacecraft to follow the same periodic halo orbit using the BCM (or any other higher fidelity model) would lead to prohibitive ΔVs. Therefore, a trajectory close to the reference periodic orbit that is natural in the new model is desired, i.e., a path that a particle would follow in the BCM without the necessity of any manoeuvres (in the case that no other perturbations or navigation errors were included). That is the so-called dynamical substitute.

In order to obtain a dynamical substitute, a series of patch points are defined along a reference trajectory. A reference path would consist of multiple revolutions of a halo orbit stacked together. Then, a multiple shooting method is applied so that the discontinuities at the patch points created when transitioning towards a new model are eliminated (method available in [14]). An example of dynamical substitute, for an L_2 NRHO of $r_p = 7000\ km$, is shown below.

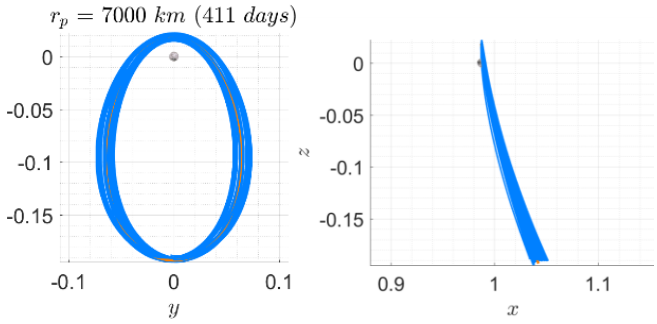

Figure 4. Dynamical substitute of a periodic L_2 halo orbit of $r_p = 7{,}000\ km$ in the BCM propagated over 411 days.

4. STATION KEEPING

A key factor to determine whether near-rectilinear orbits are viable or not as a permanent destination for the DSG is related to their orbit maintenance. Most of the motions near the collinear Lagrange points are inherently unstable, and NRHOs are not an exception. As many other orbits, they are sensitive to perturbations and some station keeping strategy is required to remain close to the nominal path. The applicability of different strategies is studied in this section. The error model used in this work is based on conservative station keeping studies in the Earth-Moon system ([5], [6], [13], [15], [16]). Regarding orbit determination errors, 1 km in position and 1 cm/s in velocity (zero mean, 3σ) is assumed. A manoeuvre execution error is also applied, which is assumed distributed according to a normal law with a typical deviation of 1% of the ΔV magnitude (1σ) and zero mean deviation. Apart from that, if the calculated manoeuvre magnitude is smaller than a threshold ($\Delta V_{min} = 0.15\ cm/s$), this is not executed. In this way, manoeuvres on the same order of magnitude as the hardware limitations are avoided.

4.1. Station Keeping Strategies

All the strategies considered have been tested using an algorithm that simulates a real-flight situation. The concept is illustrated in Figure 5. Patch points refer to the locations at which manoeuvres are applied. On the other hand, target points are defined as the aimed states after the application of every manoeuvre. Note that the target state is not necessarily the next patch point (e.g., x-cross station keeping strategy).

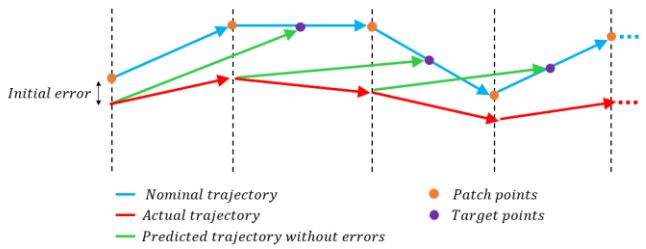

Figure 5. Schematic of the general station keeping algorithm.

The general scheme of the algorithm employed in this study is outlined below:

1. Initially, a nominal trajectory is selected.
2. Navigation errors (injection errors) are applied to the initial state or patch point.
3. The initial perturbated state is integrated using the corresponding dynamical model until the first correction manoeuvre location.
4. The required manoeuvre is determined to target some final state. Depending on the station keeping strategy considered, that state will vary, as well as the demanded ΔV. The correction is computed without taking into account any errors.
5. Apply manoeuvre execution errors to the calculated ΔV and update the current state vector. Apart from that, add navigation errors, both in position and velocity.
6. Integrate the perturbated state using the selected dynamical model until the next patch point. The patch points are defined depending on the particular station keeping strategy.
7. Check divergence. If the trajectory has diverged from the reference one, the station keeping case has failed. Otherwise, go back to step 4. A useful quantity to identify a divergent path is the momentum integral [14].

Steps 4 to 7 must be repeated until the last patch point is reached. As indicated, steps 4 and 6 are a function of the specific station keeping technique employed. Every single combination of manoeuvre determination strategy plus correction placement strategy will be labelled with a particular identifier (SKS-i). These techniques are based on three different underlying schemes; Unstable Mode Cancellation, Differential Corrections and Target Points Optimisation.

4.1.1. Unstable Mode Cancellation

Techniques under this category harness the dynamical behaviour of the trajectories in the three-body problem. The idea behind these methods is to remove the unstable component of motion to avoid asymptotical departures from the vicinity of the reference orbit.

In the context of the CR3BP, a nominal halo orbit is periodic. Then, the variational equations are linear with periodic coefficients [7], and the nonlinear system behaviour can be analysed through the eigenvalues of the STM after one period. According to Floquet theory [8], it is possible to define 6 periodic vectors related to the eigenvectors. They are the so-called Floquet modes ($\overline{e}_i$). It is clear that, due to errors in tracking, execution of maintenance manoeuvres, and inaccuracies of the dynamical model used, the spacecraft will always deviate from its nominal orbit. That deviation, δ, can be expressed in terms of the Floquet modes (Eq. (2)). The objective of this technique is to provide an impulse such that the component of the error in the unstable direction is cancelled (Eq. (3)).

$$\delta(t) = \sum_{i=1}^{6} c_i \overline{e}_i(t) \tag{2}$$

$$\delta(t) + [0 \quad 0 \quad 0 \quad \Delta V]^T = \sum_{i=2}^{6} a_i c_i \overline{e}_i(t) \tag{3}$$

On the other hand, a plan to specify the patch points along the trajectory is required. Different approaches are available. The first one is based on the monitorisation of the unstable component (c_1) of the deviation vector. Given the unstable behaviour of halo orbits, c_1 presents an exponential growth. Hence, the idea is to apply a manoeuvre every time it exceeds a maximum value ($c_{1_{max}}$). This strategy is denoted by SKS-1.

A second approach, also based on the unstable mode cancellation, consists in executing the correction manoeuvres according to a predefined schedule. Therefore, regardless of the magnitude of c_1, a velocity change is applied at the patch points. Three cases have been studied:

SKS-2: Manoeuvres are periodically applied at the apolune of the orbit.

SKS-3: Two manoeuvres are placed per orbit. In this case, they are applied at points of rotating velocity $v_y = 0$.

SKS-4: Three manoeuvres are periodically placed along the trajectory. The first one is applied at the apolune.

4.1.2. Differential Corrections

In this category, the manoeuvre placement process is the same as in the second approach of the Unstable Mode Cancellation. The difference resides in the methodology to determine the ΔVs. Now, a differential corrector is implemented to target a certain final state.

A first approach consists in defining a set of control points at regular intervals, whose position must be targeted from every previous control point. To determine the direction and magnitude of the impulsive manoeuvres, a single shooting method is used where the only free variables are the initial components of the velocity and three position constraints define the final state.

SKS-5: Manoeuvres are periodically applied at the apolune of the orbit.

SKS-6: Two manoeuvres per orbit are placed at points of $v_y = 0$.

SKS-7: Three manoeuvres per orbit, evenly distributed (in time) are periodically applied. The first one is applied at the apolune.

A second approach has been recently explored, showing promising results for NRHOs [15]. In the x-axis crossing strategy, the state at the end of each segment is defined by the x-component of the velocity in the reference orbit. Therefore, the idea is to target a reference v_x with a single shooting method. The target point is always placed at the xz-plane crossing near the perilune of the orbit since it has been observed to provide the best results [15]. On the other hand, given the sensitivity of the motion near the periapsis, the best place to apply the manoeuvre is at the apolune. This strategy is denoted by SKS-8.

4.1.3. Target Points Optimisation

For strategies under this category, the equations of motion are propagated from an initial position for a given integration period. Then, an optimisation solver is applied in order to determine the initial velocity that minimises a previously defined cost function, J. An effective approach is given in [7], where J is defined as the sum of the deviations of the predicted state vectors from the nominal orbit at specific control points plus the magnitude of the required manoeuvre (Eq. (4)). Every component of this cost function is then multiplied by a weighting matrix, which allows emphasising the most important variables of the function.

$$J = \Delta V^T Q \Delta V + \sum_{i=1}^{n} \delta r_i^T R_i \delta r_i + \delta v_i^T S_i \delta v_i \qquad (4)$$

Three control points (as recommended in [7]) evenly distributed in time have been employed, placing the third one at the next patch point. One manoeuvre at the apolune of each orbit has been employed for this strategy, which is denoted by SKS-9.

4.2. Monte Carlo Analysis

In this section, a summary of the station keeping results is presented. A Monte Carlo analysis of 250 trials has been performed, allowing for a moderate accuracy on the statistical analysis while reducing computational costs. The strategies studied in this document have been tested for a set of halo orbits from both families ranging from $r_p = 2{,}000\ km$ to $r_p = 50{,}000\ km$, emphasizing the NRHOs region.

First, results corresponding with the L_2 family are presented for the CR3BP and BCM, respectively. In every case, the yearly maintenance cost is shown. Take into account that, in the event of failure rates larger than 20% the corresponding ΔV costs have not been depicted. By inspection of Figure 6 (top), a clear trend is observed regarding the costs as a function of the periapsis radius. An increment of ΔV is observed as r_p is increased, which can be associated with the larger stability indices of these orbits. In the NRHOs region, very low station keeping costs are provided for all the strategies in the CR3BP, with practically a 0% failure rate. Moreover, the x-axis crossing approach (SKS-8) seems to be the most efficient strategy, with annual costs between 0.2 and 0.4 m/s in the zone between $r_p = 2{,}000$ and $r_p = 8{,}000\ km$. It is worth noting that after a periapsis of approximately 20,000 km to 30,000 km, all the strategies relying on a single manoeuvre per orbit cease to effectively control the spacecraft trajectory. This is due to the longer period of small halo orbits, which leads to excessive time between consecutive manoeuvres.

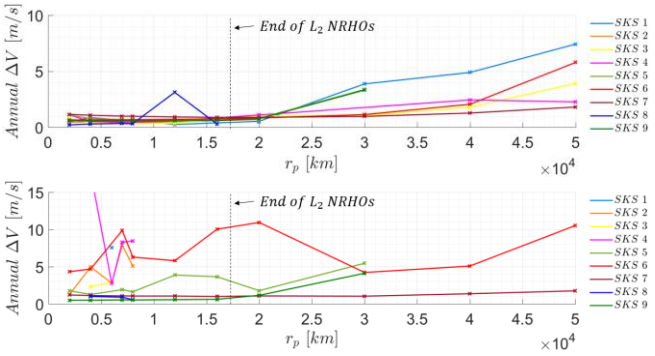

Figure 6. Station keeping results for the L_2 family in the CR3BP (top) and BCM (bottom).

Outcomes differ after the transition into the BCM. In Figure 6 (bottom), it can be appreciated that SKS-1 to SKS-4 only converge in the area of low r_p (NRHOs). However, results obtained indicate that the current implementation of the unstable mode cancellation technique is not suitable for orbits in the Earth-Moon-Sun system. Due to the Sun perturbation, the dynamical substitutes in the BCM do not follow a close path to the reference periodic orbit, and it must be noted that, in this implementation, the Floquet modes were calculated at each instant using the reference periodic trajectory (CR3BP). If the focus is placed in the remaining strategies, similar results to those from the CR3BP are obtained. As well as in the three-body problem, the x-axis crossing technique (SKS-8) only works for the NRHOs region but, unlike in Figure 6 (top), the maximum r_p for which it converges is 8,000 km. Due to the proximity of the period of nominal trajectories to a 1:3 lunar synodic resonant orbit with the Sun in the region between $r_p = 12{,}000$ and $r_p = 20{,}000\ km$, the path of the dynamical substitutes completely diverges from the reference periodic orbit [14]. This leads to important variations in the orbital characteristics from one revolution to another, which conduces to ineffective corrections. Costs are slightly increased even in the NRHO region, and the success rate is decreased. This is due to the exponential growth observed as a function of simulated time. It is relevant to point out that the mean failure time of the unsuccessful trials for $r_p = 2{,}000$, 4,000, 7,000 and 8,000 are respectively, 322, 361, 302 and 345 days. This is a clear indication that, apart from significantly reducing the annual costs (because the exponential growing region would be avoided) a success rate of zero or nearly 0% would be achieved by decreasing the simulation time to 200 – 300 days in the case of SKS-8. Finally, the robustness of strategies SKS-5, SKS-7 and SKS-9 must be highlighted.

Next, the analyses of maintenance costs for the L_1 family are exposed.

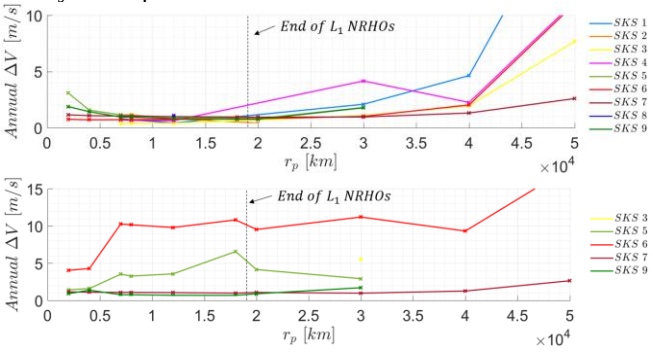

Figure 7. Station keeping results for the L_1 family in the CR3BP (top) and BCM (bottom).

At this point, it is convenient to accentuate two differences in orbital and dynamical characteristics with respect to the L_2 family; stability indices are larger for the L_1 family and, more importantly, two unstable modes coexist in a certain r_p region ($r_p = 1737$ to $r_p \approx 6600\ km$). The latter is clearly reflected in the figure above, since none of the four station keeping strategies based on the unstable mode cancellation converge for the affected periapsis radii (2,000, 4,000 and 6,000 km). One of the assumptions made to ensure the applicability of the technique is that only one unstable direction should appear, which is clearly not satisfied in the aforementioned interval. Results obtained after that region are similar to those observed in the L_2 family in the CR3BP. Generally, all the strategies behave in the same way as in the L_2 case although station keeping costs are slightly higher in the region of NRHOs. Most efficient techniques range from 0.5 to 1.2 m/s per year while in Figure 6 (top), the values are between 0.2 and 1 m/s. However, an exception is found in the SKS-8. For L_1 NRHOs with perilune radii between 2,000 and 8,000 km, the x-crossing method is ineffective for long-term station keeping. The difference in stability indices, apolune radii and period with respect the L_2 family in this region might play an important role.

Analysing the BCM results, it becomes evident the robustness of strategies SKS-5, SKS-7 and SKS-9 to efficiently control a spacecraft in both families. On the other hand, SKS-6 shows the same problems as in the orbits near the L_2 libration point, although it is a robust strategy, larger costs are obtained when implemented in the BCM.

Finally, Table 1 presents the mean computational time per iteration of all the station keeping strategies analysed in the study. Results from a single reference halo orbit are shown. However, similar trends are observed for all the members. The most computationally efficient techniques correspond to the strategies based on the unstable mode cancellation and periodical manoeuvre placement (SKS-2,3,4). These are followed by the SKS-9 (control point optimisation). On the contrary, the x-axis crossing technique (SKS-8) is the most computationally intensive.

SKS	1	2	3	4	5	6	7	8	9
CR3BP	12.0	3.4	3.6	3.5	12.3	15.1	16.7	41.9	7.1
BCM	13.6	2.1	3.4	3.0	32.5	33.6	24.8	67.1	9.3

Table 1. Computational costs of station-keeping strategies. Numerical comparison between the average computational time per iteration (measured in seconds) of the station-keeping strategies analysed in this study. All of them correspond to an L_2 halo orbit of $r_p = 7{,}000\ km$.

5. TRAJECTORY DESIGN FOR MISSIONS TO NRHOs

Another important factor to assess the feasibility of NRHOs as potential destinations for the DSG is their accessibility. First, access from the Earth is covered. Then, transfers to a Moon polar orbit are considered.

5.1. Transfer from the Earth to an NRHO

Although many types of transfers exist, the focus of this study is two-burn trajectories. An initial translunar injection manoeuvre (ΔV_{TLI}) is applied at the parking orbit and a second insertion impulse (ΔV_{INS}) is used to achieve the desired final conditions. A parking orbit of 200 km altitude is considered for all the cases evaluated in this section. Recall that other orbital elements of this orbit are not constrained (e.g., inclination) and they could have an important role regarding the overall costs. Apart from that, the two burns are always applied tangentially to the trajectory (parallel to the inertial velocity vector). Although these transfers do not guarantee the most efficient $\Delta V's$, they should provide a good approximation for the costs of these missions.

5.1.1. Fast Transfers

The DSG is part of a planned long-term crewed mission. Therefore, there is an obvious preference for short duration transfers that reduce the exposure of humans to different hazards [11]. In this section, trajectories that depart from a 200 km LEO and are inserted directly into the operational halo orbit are presented. Navigation errors are another factor that has an impact on the design of a mission. These become more critical in regions of the trajectory with high sensitivities [11], which are increased as the path approximates the primaries. Hence, insertion manoeuvres far from the Moon are preferred. For that reason, transfers tangentially arriving at the apolune of the halo orbits are first discussed. Translunar injection and insertion costs for the whole range of L_1 and L_2 halo families as a function of r_p are shown in Figure 8.

Although there is a clear dependence between the target r_p and the TLI burn, the total transfer cost is mainly determined by the halo insertion manoeuvre. Secondly, the overall cost is generally higher for the L_1 family, especially in the region of NRHOs. While the L_2 presents a minimum in the r_p range close to the NRHOs, the L_1 family shows a maximum. This leads to an approximate difference of 150

m/s in the insertion burn between both families. Taking into account the results presented so far, it can be concluded that NRHOs of both families are accessible from the Earth at reasonable costs compared to other destinations [11]. Moreover, orbits near L_2 offer better results for fast direct transfers with injection at apolune.

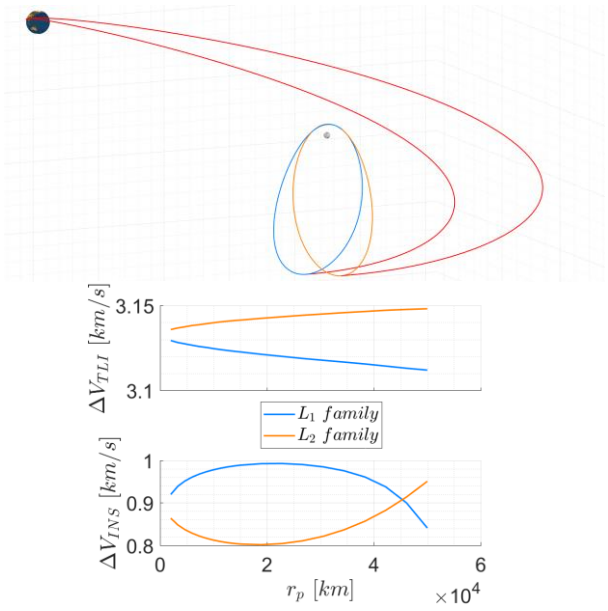

Figure 8. Direct transfers from LEO ($200x200$ km) to the apolune of halo orbits. Translunar injection and insertion costs for the whole range of L_1 and L_2 halo families as a function of r_p (bottom), and geometry of sample trajectories to NRHOs of $r_p = 6{,}000\ km$ (top) are shown.

However, it is useful to see how the costs are influenced by making the insertion in different positions along the halo orbit. A spacecraft's location within a halo orbit can be characterised according to the parameter τ. It indicates the elapsed time since the last passage through a reference point, as a fraction of the orbital period. Therefore, it ranges from 0 to 1. In this report, the reference point is taken at the apolune of the orbit, both for L_1 and L_2 families. Taking this into account, transfers to different points of the same halo orbit are depicted in Figure 9. The two halo orbits depicted have a perilune of $r_p = 45{,}000\ km$. Although this is out of the NRHOs range, transfers to halo orbits with larger r_p's are more easily converged at any τ of the orbit. Moreover, they provide valuable information that can be extrapolated to the whole halo families. In the first place, the L_2 halo orbit shows its minimum ΔV cost at the apolune ($\tau = 0$ or $\tau = 1$). Consequently, the results depicted in Figure 8 correspond with the most efficient transfers to get injected into an L_2 halo orbit, through direct fast transfers. In the second place, the opposite occurs for the L_1 family. The minimum appears at the periapsis of the orbit ($\tau = 0.5$). This indicates that, reportedly, results presented in Figure 8 can be considerably improved by placing the second burn at the perilune. In Figure 10 , transfer trajectories are analysed where the halo insertion manoeuvre is placed at $\tau = 0.5$ (perilune).

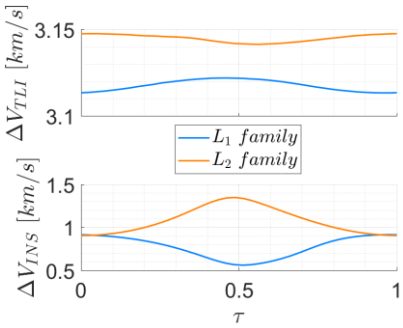

Figure 9. Direct transfers from LEO ($200x200\ km$) to arbitrary points of halo orbits. Translunar injection and insertion costs as a function of τ for halo orbits of $r_p = 45{,}000\ km$.

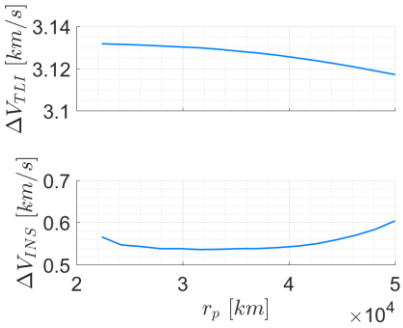

Figure 10. Direct transfers from LEO ($200x200\ km$) to the perilune of L_1 halo orbits. Translunar injection and insertion costs as a function of r_p.

As predicted, transfer costs are substantially reduced by placing the second injection manoeuvre at the perilune of the orbit. An approximate reduction between 300 and 400 m/s is observed. Unfortunately, no converged solutions have been found in the range of the NRHOs. Due to the dynamics in the vicinity of the Moon, no transfers meeting the tangential requirements at the insertion point are possible. The minimum r_p that allows a fast transfer to the perilune of the L_1 halo family using the current implementation is in the order of $20{,}000\ km$.

5.1.2. Manifold Insertion

The use of manifolds has been successfully implemented for several missions, especially in the Sun-Earth system [17], given that some of them have very close passages to the Earth, allowing for direct manifold insertions from low-Earth orbits. In the case of the Earth-Moon system, the flow around the region of interest does not yield manifolds close enough to the Earth [18], and a minimum of two manoeuvres are required to get into a halo orbit.

For this analysis, a specific operational halo orbit is studied. An NRHO with $r_p = 7{,}000\ km$ has been selected, both for L_1 and L_2 families. Initially, transfers to L_1 NRHOs are dealt with. Hence, the stable manifold associated with it

has been computed to analyse the flow near the halo orbit (Figure 11 (left)).

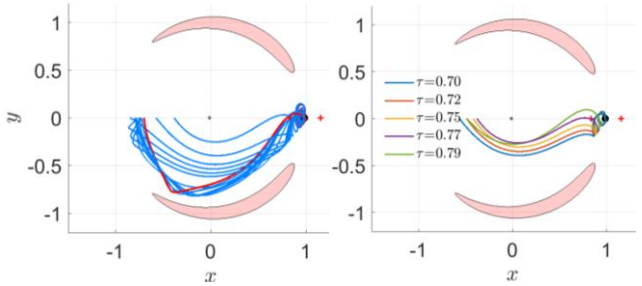

Figure 11. Stable invariant manifolds associated with an L_1 NRHO ($r_p = 7{,}000\ km$). Full discretised manifold (left) and region of the manifold yielding the closest Earth approach (right).

Potential manifold candidates for low-cost transfers should have a periapsis with a close passage to the Earth [14]. In addition, an efficient trajectory should connect the LEO to the corresponding apogee of the manifold [14]. Considering this, the range of possible τ's can be restricted to those which lead to low perigees, which have been isolated in Figure 11 (right). All these manifolds also share a common geometry in the zone near the second primary. The relation between t_m and the costs near the first apogee associated with the manifolds shown in Figure 11 is depicted in Figure 12. As expected, all the cases present a minimum in the t_m span covered. In addition, manifolds with lower perigees present lower costs. It can be concluded that clear benefits are obtained through the exploitation of stable manifolds for an L_1 NRHO. A good strategy has been identified to determine efficient transfers to this type of orbits, and approximate savings of 400 to 500 m/s are achieved with respect to fast transfers. The main drawback is the higher transfer times with respect to direct trajectories.

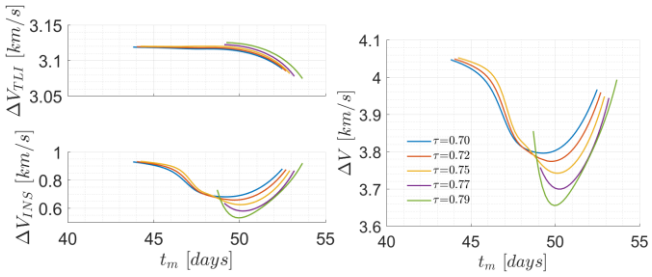

Figure 12. Transfer costs near the first apogee of invariant manifolds (L_1 NRHO of $r_p = 7{,}000\ km$). The manifolds analysed correspond to those depicted in Figure 11 (right).

Next, the case of L_2 NRHOs is addressed. It is observed that only exterior manifolds exist for the r_p chosen. Therefore, only transfers with insertion manoeuvres placed in the exterior realm are possible. ΔV costs can be slightly improved with respect to direct fast transfers. However, due to the large increase in the TOF, a trajectory of these characteristics is not convenient. Hence, a fast transfer appears to be the best option for an L_2 NRHO in a two-burn scenario.

5.1.3. Complex Transfer: Halo Insertion plus Transfer to NRHO

As an alternative to the transfer issues for L_2 NRHO as described above, this section proposes to exploit the highly unstable character of classical halo orbits. The concept is to efficiently transfer from an LEO to an *auxiliary* standard halo orbit as a previous step to a low-cost transfer between two halo orbits.

For the transfer between the halo orbits, it is suggested to construct a transfer trajectory by connecting the unstable manifold of the auxiliary halo orbit to the stable manifold of the final NRHO. Poincaré maps are commonly used to characterise the behaviour of groups of trajectories [19]. However, a vastly different and efficient technique is developed in [20], which was considered more appropriate given the properties of the orbit of this study. The difference with other techniques lies in the methodology used to identify the specific manifolds that would lead to small transfer costs, which is based on two-body dynamics.

The total cost of the transfer can be minimised by searching for manifolds with similar characteristics (shape and orientation). The shape and orientation of a trajectory near a primary body can be quantified through two parameters associated with the two-body problem; the normalized angular momentum vector, $\vec{h}_{norm}$, and the eccentricity vector, $\vec{e}$ [20]. Every point along a trajectory can be characterised by these two vectors. However, it must be ensured that the position is close enough to the primary so that the two-body problem assumption is valid. Hence, given two points (one from each manifold), the difference between the two vectors defined above determines how well they match in orientation and shape. This information can be expressed in terms of a single parameter as

$$\kappa = \left|\vec{h}_{norm_s} - \vec{h}_{norm_u}\right| + \left|\vec{e}_s - \vec{e}_u\right| \qquad (5)$$

It can be shown that the transfer cost (ΔV) and κ are linearly dependent [20]. So, a search is needed to find the combination of manifolds that gives the lowest κ. Once the right pair of manifolds has been identified, the next step is to find the optimum bridge that connects both trajectories (Figure 13).

The method explained above has been used to quantify the costs of a transfer to an NRHO of $r_p = 7{,}000\ km$ from highly unstable halo orbits (Figure 14 (left)). The resulting geometry for the specific case of $r_p = 40{,}000\ km$ is shown in Figure 14 (right). Highly efficient transfers exist ($\Delta V < 60\ m/s$) to an NRHO of 7,000 km. However, as it is shown in Figure 14, costs are rapidly incremented as the periapsis radius of the initial unstable orbit is increased. Therefore, an r_p as low as possible is desired for the staging orbit. The proposed method (using normal halo as staging orbit) will be

beneficial if efficient transfers to these auxiliary orbits are available, which is analysed next.

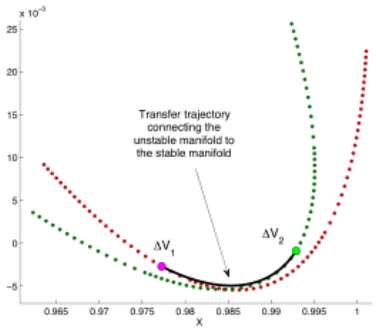

Figure 13. Transfer between halo orbits schematic: The first maneuver on the unstable manifold (pink circle), targets a state on the stable manifold. The second maneuver (green circle), corrects the velocity at the end of the bridging trajectory (black) [20].

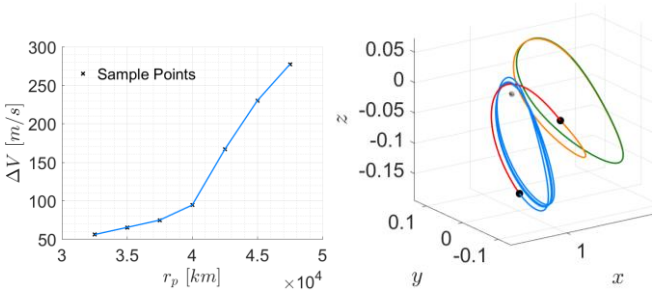

Figure 14. Total costs to transfer from a normal halo orbit to an NRHO as a function of the r_p of the initial orbit (left) and sample trajectory (right). Different segments are identified; halo orbits (green), unstable manifold of the small halo orbit (orange), stable manifold of the NRHO (blue) and bridge segment (red). The halo orbits periapsis radii are 40,000 and 7,000 km.

Unlike for L_2 NRHOs, classical halo orbits possess interior manifolds that depart towards the Earth. The minimum r_p that has allowed the exploitation of the interior stable invariant manifolds is $35{,}000\ km$. Minimum costs to reach auxiliary halo orbits of different periapsis are presented in the following table.

$r_p\ [km]$	$\Delta V_{TLI}\left[\frac{km}{s}\right]$	$\Delta V_{INS}\left[\frac{km}{s}\right]$	$t_m[days]$
35,000	3.035	0.583	54.6
37,500	3.037	0.565	54.6
40,000	3.032	0.616	47.9
42,500	3.033	0.600	45.4
45,000	3.033	0.587	43.6
47,500	3.033	0.591	43.0

Table 2. Optimum costs and manifold propagation from a LEO (200x200 km) to of a set of halo manifolds.

Finally, the total costs to transfer from the Earth to an L_2 NRHO using the complex transfer is computed combining costs of Table 2 and Figure 14. Maximum savings with respect to fast transfers in the order of $250\ m/s$ are achievable.

5.2. Transfer from an NRHO to a Circular Moon Orbit

An important application of the DSG is to facilitate landing missions to the Moon's surface. Particularly, polar regions are of great interest due to recent findings of abundant ice in shadowed areas of the Moon [21]. Therefore, accessibility to these zones is analysed in this section.

The descent from the NRHO to the landing site will be carried out in different phases [1]. Initially, the spacecraft will be transferred from the NRHO to a polar circular parking orbit around the Moon. Subsequently, an impulsive manoeuvre will be applied to lower the periapsis of the orbit. Finally, when the perilune is reached, a landing phase with variable thrust is performed. For the purposes of this investigation, only the analysis of the first phase is considered useful. Both the second and third steps only depend on the circular parking orbit (CLMO). Therefore, only transfer costs to reach the CLMO are presented and compared with those from other cislunar orbits.

The strategy followed to determine the transfer trajectories is the same as for direct transfers from an LEO to an NRHO. It should be noted, however, that the parking orbit constraints are now referred to the CLMO, and the state vector must be computed relative to the Moon. Also, given the special interest for the polar regions, an inclination constraint has been added to target a polar orbit ($i = 90°$). Apart from that, it has been considered appropriate to remove the tangency constraint at the NRHO since convergence issues have been observed for some cases. Results obtained to transfer from an NRHO of $r_p = 7{,}000\ km$ to a CLMO of $300\ km$ altitude are presented below.

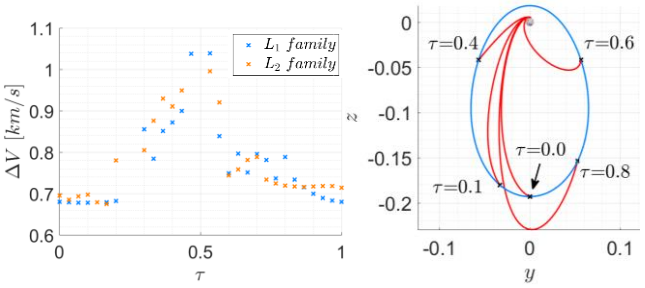

Figure 15. Costs to transfer from an NRHO ($r_p = 7{,}000\ km$) to a polar CLMO ($300x300\ km$) as a function of τ (left), and geometry of different transfers for the L_2 NRHO (right).

According to Figure 15, the optimal τ to transfer from the NRHO to a CLMO is $\tau = 0$ or close to 0. That corresponds with the apolune of the orbit for both L_1 and L_2 halo families. On the contrary, transferring from the perilune ($\tau = 0.5$) entails the largest ΔV's. These results demonstrate the availability of efficient transfers connecting the near-rectilinear halo orbits and the polar regions of the Moon (recall that all the transfers are injected into a circular orbit of

$i = 90°$). Whitley et al. [22] provide with a general estimation of the costs to access the lunar poles from different orbits of the cislunar space. It is worth noting that all the alternatives to the NRHOs are more expensive in terms of ΔV. (e.g., 830 m/s for Distant Retrograde Orbits and 800 m/s for L_2 halo orbits against <700 m/s for NRHOs). Another advantage of the NRHOs with respect to the alternatives is that, due to their close passage to the Moon, the TOF can be considerably reduced (from 4 to ~0.5 days) if needed [14]. This should be done at expenses of an increased ΔV (~800 m/s).

6. CONCLUSION

The present study has focused on the assessment of station keeping costs and the availability of efficient transfers from the Earth and the Moon to the NRHOs and vice versa.

A variety of station keeping strategies have been proposed to control a spacecraft in halo orbits, paying particular attention to NRHOs. Two robust techniques, one based on differential corrections (position targeting; SKS-5, 6, 7) and another one based on a control-point optimisation scheme (SKS-9), have been identified. SKS-5 and SKS-9 are especially optimal for NRHOs station keeping, requiring a single manoeuvre per orbit. The latter has demonstrated to be more efficient in terms of computational and annual ΔV costs. As an approximation, a ΔV of $0.5\ m/s$ is required per year in an L_2 NRHO. It has also been observed that, generally, maintenance costs are slightly higher in orbits near the L_1 point ($\sim 1\ m/s$ for NRHOs). The most efficient station keeping results have been provided by the x-axis crossing technique ($\sim 0.25\ m/s$ for L_2 NRHOs). However, after the transition to the BCM, costs are increased to some extent ($\sim 0.8\ m/s$) due to an exponential growth of the ΔV requirements at the end of the simulations. Also, the x-axis crossing technique is valid only for orbits with a perilune radius smaller than $12{,}000\ km$ for the L_2 family, and it is ineffective for the whole L_1 family.

The second goal of this study is to demonstrate the availability of efficient transfers connecting the NRHOs with other dynamical structures in the cis-lunar space and beyond. The CR3BP has been considered a powerful tool for this early phase of trajectory design. First, feasible direct and fast transfers from the Earth, crucial for crewed missions, have been evidenced for both L_1 and L_2 NRHOs, being cheaper in the case of L_2 family. By allowing the TOF to be increased, very efficient transfers are found for L_1 NRHOs by exploiting their stable invariant manifolds. The dynamical flow associated with L_2 NRHOs does not allow to directly leverage their manifolds. Nevertheless, a technique has been presented to reduce transfer costs from the Earth by using the stability properties of other halo members of the same family. Finally, a study has been performed to compute efficient trajectories from a NRHO to the Moon and vice versa, showing promising results with respect to other dynamical structures in the cislunar space.

7. REFERENCES

[1] ESA, "GNC preliminary design for rendezvous and docking in NRO orbits around the Moon, statement of work, ESA ITT AO/1-9173/17/NL/CRS," 2017.

[2] E. Mahoney, "Scientists Share Ideas for Gateway Activities Near the Moon," 2018. [Online]. Available: https://www.nasa.gov/feature/scientists-share-ideas-for-gateway-activities-near-the-moon. [Accessed: 28-Apr-2018].

[3] D. C. Davis, S. M. Phillips, K. C. Howell, S. Vutukuri, and B. P. Mccarthy, "Stationkeeping and Transfer Trajectory Design for Spacecraft in Cislunar Space," *Adv. Astronaut. Sci.*, pp. 1–20, 2017.

[4] M. Woodard, D. Folta, and D. Woodfork, "ARTEMIS: The First Mission to the Lunar Libration Orbits," *Electron. Publ.*, no. 1, pp. 6–8, 2007.

[5] D. C. Davis *et al.*, "Orbit maintenance and navigation of human spacecraft at cislunar near rectilinear halo orbits," *Adv. Astronaut. Sci.*, vol. 160, pp. 2257–2276, 2017.

[6] M. Shirobokov, S. Trofimov, and M. Ovchinnikov, "Survey of Station-Keeping Techniques for Libration Point Orbits," *J. Guid. Control. Dyn.*, vol. 40, no. 5, pp. 1085–1105, 2017.

[7] K. C. Howell and T. M. Keeter, "Station-keeping strategies for libration point orbits. Target point and floquet modes approaches." 1995.

[8] G. Gomez, J. Llibre, R. Martínez, and C. Simó, *Dynamics and Mission Design Near Libration Points, Volume I Fundamentals: The Case of Collinear Libration Points*. World Scientific Publishing Company, 2001.

[9] W. S. Koon, M. W. Lo, J. E. Marsden, and S. D. Ross, "Dynamical systems, the three-body problem and space mission design," p. 312, 2008.

[10] G. Gomez, J. Llibre, R. Martínez, and C. Simó, *Dynamics and Mission Design Near Libration Points, Volume II Fundamentals: The Case of Triangular Libration Points*, 1st ed., vol. 2. World Scientific Publishing Company, 2001.

[11] E. M. Zimovan, K. C. Howell, and D. C. Davis, "Near Rectilinear Halo Orbits and Their Application in Cis-Lunar Space," *3rd IAA Conf. Dyn. Control Sp. Syst. (DyCoSS), Moscow, Russ. May 30-June 1, Pap. IAA-AAS-DyCoSS3-125*, p. 20, 2017.

[12] C. E. Patterson, "Representations of invariant manifolds for applications in system-to-system transfer design," Purdue University, 2005.

[13] D. J. Grebow, M. T. Ozimek, K. C. Howell, and D. C. Folta, "Multi-body orbit architectures for lunar south pole coverage," *Adv. Astronaut. Sci.*, vol. 124 II, pp. 1285–1307, 2006.

[14] C. Sánchez, "Preliminary Design of Near Rectilinear Orbits around the Moon as Operational Orbit for the Future Deep Space Gateway," Cranfield University, 2018.

[15] D. Guzzetti, E. M. Zimovan, K. C. Howell, and D. C. Davis, "Stationkeeping analysis for spacecraft in lunar near rectilinear halo orbits," *Adv. Astronaut. Sci.*, vol. 160, pp. 3199–3218, 2017.

[16] T. a Pavlak and K. C. Howell, "Strategy for Optimal , Long-Term Stationkeeping of Libration Point Orbits in the Earth-Moon System," *AIAA/AAS Astrodyn. Spec. Conf.*, no. August, pp. 1–16, 2012.

[17] J. S. Parker and G. H. Born, "Direct lunar halo orbit transfers," *J. Astronaut. Sci.*, vol. 56, no. 4, pp. 441–476, 2008.
[18] R. R. Rausch, "Earth To Halo Orbit Transfer Trajectories," Purdue University, 2005.
[19] D. C. Davis and K. C. Howell, "Long-term evolution of trajectories near the smaller primary in the restricted problem," *Adv. Astronaut. Sci.*, vol. 136, no. September, pp. 1277–1296, 2010.
[20] K. E. Davis, R. L. Anderson, D. J. Scheeres, and G. H. Born, "Connecting libration point orbits of different energies using invariant manifolds," *Adv. Astronaut. Sci.*, vol. 134, pp. 2367–2386, 2009.
[21] J. Dino, "LCROSS Impact Data Indicates Water on Moon," 2009. [Online]. Available: https://www.nasa.gov/mission_pages/LCROSS/main/prelim_water_results.html. [Accessed: 26-Aug-2018].
[22] R. Whitley and R. Martinez, "Options for staging orbits in cislunar space," *IEEE Aerosp. Conf. Proc.*, vol. 2016–June, 2016.

Near rectilinear orbits around the moon as operational orbit for the future deep space gateway

Sánchez Lara, Carlos

2018-11-09

Carlos Sánchez Lara and Joan Pau Sánchez Cuartielles. Near rectilinear orbits around the moon as operational orbit for the future deep space gateway. Proceedings of the 7th International Conference on Astrodynamics Tools and Techniques (ICATT), 6-9th November 2018, Oberpfaffenhofen, Germany.

https://indico.esa.int/event/224/contributions/4010/